

Distribution Agreement

In presenting this thesis as a partial fulfillment of the requirements for a degree from Emory University, I hereby grant to Emory University and its agents the non-exclusive license to archive, make accessible, and display my thesis in whole or in part in all forms of media, now or hereafter now, including display on the World Wide Web. I understand that I may select some access restrictions as part of the online submission of this thesis. I retain all ownership rights to the copyright of the thesis. I also retain the right to use in future works (such as articles or books) all or part of this thesis.

Ran Tao

April 8, 2021

Flow and clogging of soft particles in 2D hoppers

by

Ran Tao

Dr. Eric R. Weeks
Adviser

Physics Department

Dr. Eric R. Weeks
Adviser

Dr. Effrosyni Seitaridou
Committee Member

Dr. Suresh Venapally
Committee Member

2021

Flow and clogging of soft particles in 2D hoppers

By

Ran Tao

Dr. Eric R. Weeks

Adviser

An abstract of
a thesis submitted to the Faculty of Emory College of Arts and Sciences
of Emory University in partial fulfillment
of the requirements of the degree of
Bachelor of Science with Honors

Physics Department

2021

Abstract

Flow and clogging of soft particles in 2D hoppers

By Ran Tao

I study the outflow of soft particles through quasi-two-dimensional hoppers with both experiments and simulations. The experiments utilize spheres made with soft hydrogel, silicone rubber and glass. The hopper chamber has an adjustable exit width and tilt angle (the latter to control the magnitude of gravitational forcing). My simulation mimics the experiments using purely two-dimensional soft particles with viscous interactions but no friction. Results from both simulations and experiments demonstrate that clogging is easier for reduced gravitational force or stiffer particles. For particles with low or no friction, the average number of particles in a clogging arch depends only on the ratio between hopper exit width and particle's diameter. In contrast for the silicone rubber particles with larger frictional interactions, arches are larger than the low friction case. Additionally, an analysis of the number of particles left in the hopper when clogging occurs provides evidence for a hydrostatic pressure effect that is relevant for the clogging of soft particles, but not so for the harder (glass) or frictional (silicone rubber) particles. Through simulations, I also studied the flux of soft particles flowing through two-dimensional hoppers. I derived a flux law to describe the flux under different gravitational conditions and varying exit width. The flux law agrees with simulation data except when the exit width is too large.

Flow and clogging of soft particles in 2D hoppers

By

Ran Tao

Dr. Eric R. Weeks

Adviser

A thesis submitted to the Faculty of Emory College of Arts and Sciences
of Emory University in partial fulfillment
of the requirements of the degree of
Bachelor of Science with Honors

Physics Department

2021

Table of Contents

Introduction	1
Experimental Methods.....	2
Simulation Methods	6
Results	8
Conclusion	25
Bibliography.....	27

Table of Figures and Tables

Figure 1: Photograph of different types of particles in a clogged state	3
Figure 2: Plot of the Young's modulus for hydrogel particles with different sizes	5
Table 1: Properties of different types of particles	6
Figure 3: Experimental probability of clogging	8
Figure 4: Clogging probability and Gompertz distribution for fixed driving force in simulation.....	10
Figure 5: Clogging probability and Gompertz distribution for fixed opening width in simulation	11
Figure 6: Sigmoid fit parameters.....	12
Figure 7: Hazard rate and Gompertz distribution	14
Figure 8: Histograms of probability of clogging with a certain number of particles left in the hopper.....	17
Figure 9: Average arch size in simulation and experiments.....	19
Figure 10: Simulation data of flux	21
Figure 11: Fitting of simulation data.....	22
Figure 12: Analysis of α and a	23
Figure 13: Comparison between simulation data and the flux law	24
Figure 14: Average velocity in y direction and density for $g = 0.001$ and $w = 12$	25
Figure 15: Average velocity in y direction and density for $g = 0.005$ and $w = 15$	26

I. INTRODUCTION

The hopper discharge of granular materials has been intensively studied due to its practical importance to industries, such as agriculture, architecture, and mining [1–6]. Hoppers are containers with funnel-shaped bottoms where particles can flow out. By adjusting the opening size, the flow rate can be controlled [5]. However, at small opening sizes, clogging can occur, in particular if the particles can form an arch that spans the opening size [7]. This typically happens at a critical opening size of about 3 to 6 particle diameters [1, 3, 5, 8–11]. Even when the opening size is greater than the critical size, the flow rate fluctuates due to transient clogging events [12, 13], so understanding the clogging process is important when dispensing granular materials out of a hopper. Even in everyday life, knowledge of the flow of granular materials has been applied to the study of emergency evacuations of people out of a room [14–16]. There are already many prior studies on the flow and clogging of hard particles. However, the outflow of soft particles still lacks a comprehensive physical description.

Prior work showed the importance of softness to the clogging process. Experiments showed that due to soft particles' ability to deform, clogging only occurred for much smaller opening widths compared with results from the studies of hard particles [17, 18], which significantly changed the flow rate [19, 20]. Slightly above the critical opening size, there could be long-lived transient clogs that nonetheless unclogged [13]. For even larger opening sizes, it was found that the flow rate and internal velocity fields differ for soft particles compared to hard particles [13, 21, 22]. Simulations of soft frictionless granular materials demonstrate that clogging is easier for stiffer particles or with weaker gravitational forces [19]. The prior experimental studies of soft particles mostly focused on hydrogel particles [13, 19–22] although one study also included oil particles [19] which, due to their easy ability to deform, were even harder to clog.

In this honor thesis, I study clogging in the outflow of a hopper using a quasi-two-dimensional experiment with granular materials with varying softness, and simulations mimicking frictionless soft particles. My experiment uses glass particles, silicone rubber particles, and hydrogel particles, as shown in Fig. 1. The hopper can be tilted relative to gravity, allowing us to adjust the driving force. These particle choices and tilt angles allow us to vary the particle effective stiffness by a factor of 10^4 . For the harder particles (glass, silicone

rubber; lower gravity) clogging is easier and occurs with larger opening widths; for the softer hydrogel particles the opposite is true. The simulation results agree with the experimental clogging probabilities with no adjustable parameters. Both the experiment and simulations show that the number of particles forming the arch is determined by the ratio between the opening width and the particle diameter regardless of the particle softness. The sole exception is for the silicone rubber particles, which have a markedly higher friction coefficient leading to larger arches. In addition, an examination of the number of particles in the hopper when a clog occurs reveals that the hydrostatic pressure of the soft particles causes clogging to be less likely when the hopper is full, and exponentially more likely as the hopper drains. The exceptions are for the glass particles and silicone rubber particles, suggesting hardness and friction change the physics of soft particle clogging. Finally, inspired by Beverloo's law which studies the flow rate of hard particles through orifices [5], I do simulations to derive a flux law to describe the flow of soft particles in two-dimensional hoppers. The flux law matches with simulation data except when the opening exit width is too large.

II. EXPERIMENTAL METHODS

The apparatus used in my experiment is the same as the one described in our group's prior work [19]; I reprise the key details here. The hopper has two movable sidewall blocks at 34° angles with respect to the horizontal, pictured in Fig. 1. Above and below the main hopper chamber there are two identical storage chambers. Before I start the experiment, I place 200 particles in the upper storage chamber. A bottom metal plate inserted between the upper storage chamber and the hopper holds these particles. To begin the experiment, I rapidly remove the metal plate by hand allowing the particles to fall. Particles that fall through the hopper are collected by the storage chamber below the hopper. The two storage chambers are then swapped, moving the particles back to the top position, readying for the next trial. If a clog occurs, the opening width is increased to let those particles drain out. To ensure a reproducible opening width between trials, the hopper blocks are pushed against an inserted plastic spacer with the desired opening width and then locked into place. The entire apparatus is mounted on a horizontal axis, so that I can vary the component of the gravitational force in the plane of the hopper by setting the tilt angle θ relative to the horizontal. In practice, I vary the component of gravity in the hopper by a factor of 6. At

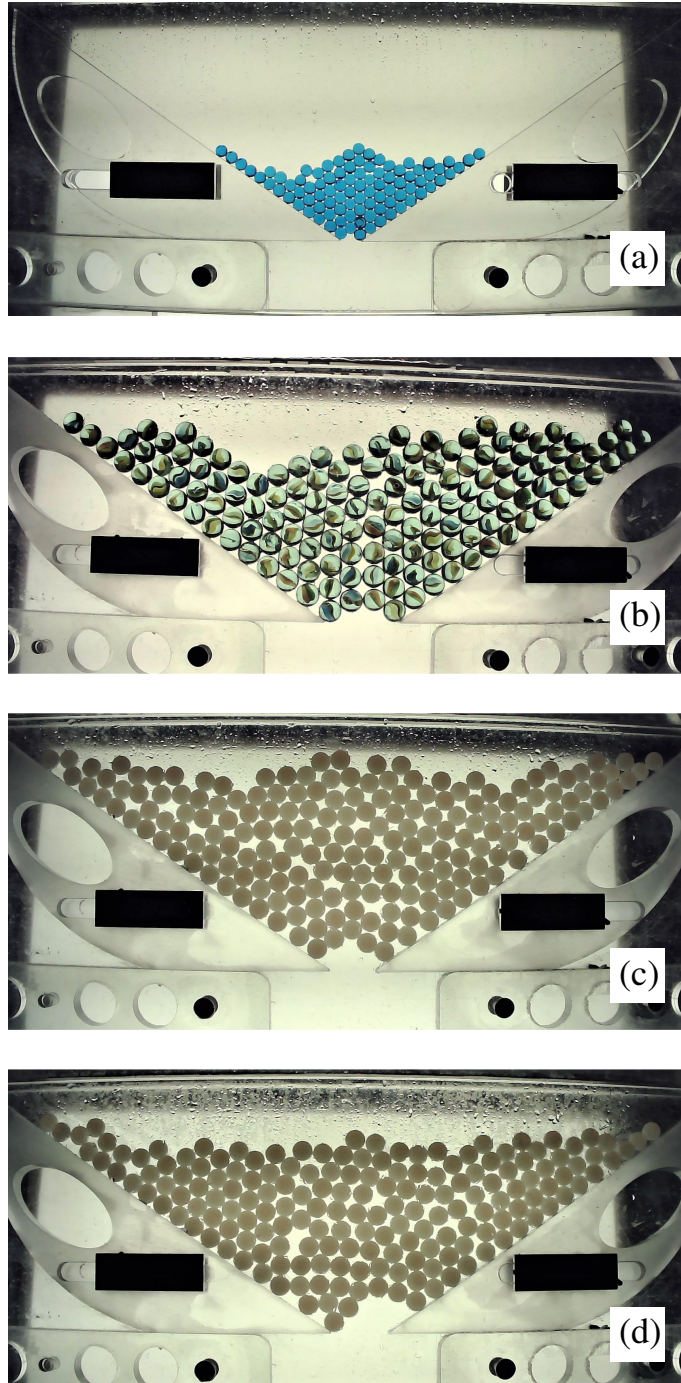


FIG. 1: Photograph of different types of particles in a clogged state, with the sample chamber fully vertical (maximum force of gravity). (a) Clogging of small hydrogel particles, showing a 3 particle arch. The opening width is $w = 14.3 \text{ mm} = 1.81d$ in terms of the mean particle diameter $d = 7.9 \text{ mm}$. (b) Clogging of glass spheres, showing a 4 particles arch with $w = 51.5 \text{ mm} = 3.32d$, $d = 15.5 \text{ mm}$. (c) Clogging of silicone rubber particles, showing a 5 particle arch with $w = 30.6 \text{ mm} = 2.19d$, $d = 14.0 \text{ mm}$. (d) Clogging of silicone rubber particles, showing a 6 particle arch with $w = 39.9 \text{ mm} = 2.85d$.

the smallest tilt angles, occasionally particles get stuck between the bottom of the upper storage container and the top of the hopper, on the seam between the two parts of the experiment. Accordingly, I avoid tilt angles where this problem occurs, which is the limiting factor on my ability to adjust the gravitational force.

I use three types of particles with varying softness in the clogging experiments: soft hydrogel particles, silicone rubber particles, and glass particles. The physical properties of the particles are given in Table I. The hydrogel particles are a polyacrylamide gel (blue water beads, purchased from AINOLWAY, Amazon.com). When these hydrogel particles are dry, they are spheres with diameters around 3 mm and moderate polydispersity. I use two sieves to constrain the dry particle diameter to be between 2.80 mm and 3.15 mm. I then swell the hydrogel particles in salt water; by changing the concentration of salt, I can control the final diameter of the hydrogel particles. By measuring the Young's modulus of hydrogel particles with varying radius, I find that hydrogel particles with smaller radius are harder than hydrogel particles with larger radius. The data is shown in Fig. 2. Salt water with concentration 0.01 mole/L swells the hydrogel particles to a mean diameter of 13.8 mm, and a concentration of 0.5 mole/L results in a mean diameter of 7.9 mm. I can adjust the thickness of the sample chamber, to 17.0 mm and 9.0 mm respectively for the large and small hydrogel particles. Additionally, I use silicone rubber particles with diameters 14.0 mm (purchased from Hebei Baorui Rubber Products Company, Alibaba.com), and glass particles with diameters 15.5 mm (marbles purchased from Amazon.com). The rubber and glass particles are used in sample chambers with thickness 17.0 mm.

To measure the physical properties of my hydrogel and silicone rubber particles, I use a TA Instruments AR2000 rheometer with a parallel-plate geometry. To measure the Young's modulus of the hydrogel particles and the silicone rubber particles, I compress individual spheres and measure the normal force. The resulting relation between the compression force and the displacement is well fit by the Hertzian force law. Using a Poisson ratio of 0.3 [19, 23], I determine the Young's modulus; the data are listed in Table I. The small and large hydrogel particles come from the same dry particles, so accordingly the larger elastic modulus of the smaller particles (swelled in high concentration salt water) is due to the higher polymer concentration of the smaller hydrogel particle. The glass particles are too stiff to be measured in the rheometer, so the quoted modulus is an estimate (from https://www.engineeringtoolbox.com/young-modulus-d_417.html); the main point is that

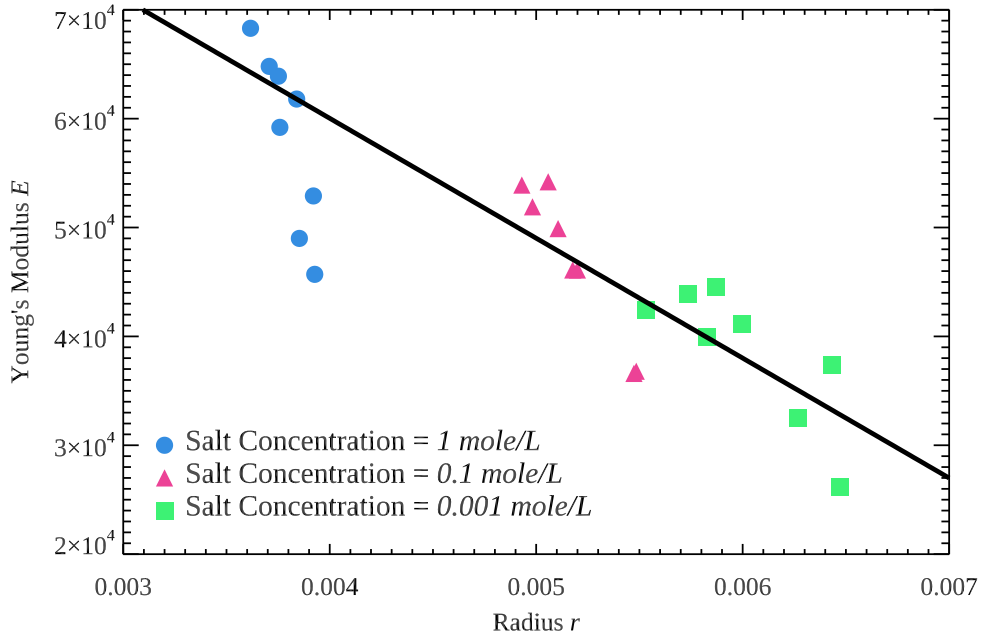


FIG. 2: Plot of the Young's modulus for hydrogel particles with different sizes. Different symbols represent data collected from hydrogel particles submerged in salt water with different concentrations. The salt concentration affects the size of hydrogel particles and larger hydrogel particles are softer.

the elastic modulus of glass is several orders of magnitude larger than the other particle types.

To measure the surface friction of the particles, I use the technique described in our group's prior work [19]. Briefly, I place a pair of particles symmetrically a distance $R = 1$ cm from the rheometer axis. The particles are trapped in small wells made from glue and paper to prevent the particles from rolling. The parallel plate rheometer tool compresses the particles slightly with normal force N , and I then measure the torque τ required to rotate the rheometer tool. The friction coefficient is then calculated from $\mu = \tau/2NR$. The results depend somewhat on the rotation speed [24], so I have uncertainties of 50% listed in Table I for all but glass (where the results vary less). The main point made in Table I is that the silicone rubber particles have a clear friction coefficient about 50 – 100 times larger than the other particle types.

To look for clogging, I load the hopper with 200 particles and allow them to flow through the hopper with a fixed opening width. I record whether the experiment clogs. If a clog occurs, I wait at least a minute to confirm the particles are stationary; in practice any

Particle	d (mm)	E (kPa)	μ
large hydrogel	13.8 ± 0.6	49.1 ± 5.8	0.004 ± 0.002
small hydrogel	7.9 ± 0.2	55.0 ± 4.5	0.004 ± 0.002
silicone rubber	14.0 ± 0.1	4600 ± 100	0.4 ± 0.2
glass	15.5 ± 0.1	$(7 \pm 2) \times 10^7$	0.009 ± 0.002

TABLE I: The diameter d , Young’s modulus E , and coefficient of sliding friction μ for each particle type. The large hydrogel particles are made by swelling the dry particles in 0.01 M NaCl, while the small hydrogel particles use 0.5 M NaCl.

transient clogs last only a few seconds, in agreement with our group’s prior experiments [19] and observations by Harth *et al.* [13]. Clogging probabilities are measured by repeating each condition at least 20 times.

III. SIMULATION METHODS

In addition to the experiments, I also do simulations using the two-dimensional Durian Bubble Model [25, 26] as modified in our group’s prior work [19]. Dr. Eric R. Weeks wrote the original simulation code and generated some data used in the honor thesis. After modifying the code, I generated and analyzed other data involved in this thesis. I briefly reprise the details of Ref. [19] here. This model assumes strong viscous forces such that the velocity-dependent viscous forces are balanced by all other forces, and thus at each time step a differential equation is solved for the velocity rather than the acceleration. This differential equation for each particle i is:

$$\sum_j [\vec{F}_{ij}^{\text{contact}} + \vec{F}_{ij}^{\text{visc}}(\vec{v}_i, \vec{v}_j)l] + \vec{F}_i^{\text{wall}} + \vec{F}_i^{\text{grav}} - \vec{F}_i^{\text{drag}}(\vec{v}_i) = 0. \quad (1)$$

Each soft particle has a radius R_i and the contact force is zero if two particles do not overlap. For overlapping particles i and j , the contact force is given by

$$\vec{F}_{ij}^{\text{contact}} = F_0 \left[\frac{1}{|\vec{r}_i - \vec{r}_j|} - \frac{1}{|R_i + R_j|} \right] \vec{r}_{ij}, \quad (2)$$

based on their positions \vec{r} , defining their separation as $\vec{r}_{ij} = \vec{r}_j - \vec{r}_i$, and requiring $|\vec{r}_{ij}| < (R_i + R_j)$ for overlaps. The viscous force is experienced by overlapping particles moving

at different velocities and is given by $\vec{F}_{ij}^{\text{visc}} = b(\vec{v}_i - \vec{v}_j)$. The wall force is a contact force experienced by particles which overlap the wall, treating the wall as a particle with $R_j = 0$ in Eqn. 2. The gravitational force is $F_i^{\text{grav}} = -\rho g R_i^2 \hat{y}$, proportional to the particle radius. This model was inspired by experiments with oil particles compressed between two parallel plates [19], so the final force is a drag force coming from these plates, $F_i^{\text{drag}} = -c R_i^2 \vec{v}_i$. I set $F_0 = b = c = \rho = 1$ and vary g to influence the importance of particle softness. The mean particle radius $\langle R \rangle$ is set to be 1 and is our unit of length. The unit of time is $b\langle R \rangle / F_0$, which is the time scale for two particles to push apart, limited by inter-particle viscous interactions. With these parameter choices, the free-fall velocity of an isolated particle is g . See Ref. [19] for further discussion about these parameter choices.

The specific geometry is matched to the experiment, with a hopper wedge angle of 34° . I simulate 800 particles with a polydispersity of 0.1 (the polydispersity is the standard deviation of R_i divided by $\langle R_i \rangle = 1$). The particles are initialized in random positions above the hopper exit, and then allowed to fall toward the exit. Equation 1 is computed using the 4th order Runge-Kutta algorithm with a time step of 0.1, except for the simulations with $g = 10^{-4}$ where a time step of 1.0 is used. In some cases, the simulation ends with all of the particles falling out of the hopper, defining a situation without a clog. In other cases, the simulation is ended when the maximum speed of all particles in the hopper falls below 10^{-10} , defining a clog. In practice, once the maximum velocity of the particles in the hopper is below 10^{-6} , their velocities decay exponentially toward zero; the particles do not unclog [19]. Stated another way, I do occasionally observe long transient clogs where the particles have slight motions and eventually unclog, and these transients always have a maximum velocity of at least one particle above 10^{-6} , allowing for the rearrangements necessary to unclog and returning to a flowing state.

To study the flow rate of soft particles in 2D hoppers, I do the same simulation with exit opening widths chosen greater than the critical opening size so that permanent clogging does not occur. The simulation starts when all particles are stable in the hopper, which means that their maximum velocity at the beginning of the simulation is below 10^{-2} . The simulation records the flux and the number of particles remaining in the hopper. For specific opening width and gravitational condition, I repeat the simulation 10 times trying to derive a flux law for the outflow of soft particles under different situations.

IV. RESULTS

A. Clogging Probability

Our first goal is to investigate the clogging probability. The experimental data are shown in Fig. 3. I repeat each experimental condition 20 times and compute the clogging probability P_{clog} from the fraction of times that I observe clogging. I go through the same process for different types of particles, different values of opening width w , and a variety of hopper tilt angles θ . Each set of symbols illustrates that P_{clog} decreases as I enlarge the hopper opening width for a fixed gravitational force. The maximum uncertainty of clogging probability occurs at $P_{\text{clog}}=0.5$, where we have a ± 0.11 uncertainty for 20 trials. Overall, these results are consistent with our group's prior experimental work with slightly different hydrogel particles [19].

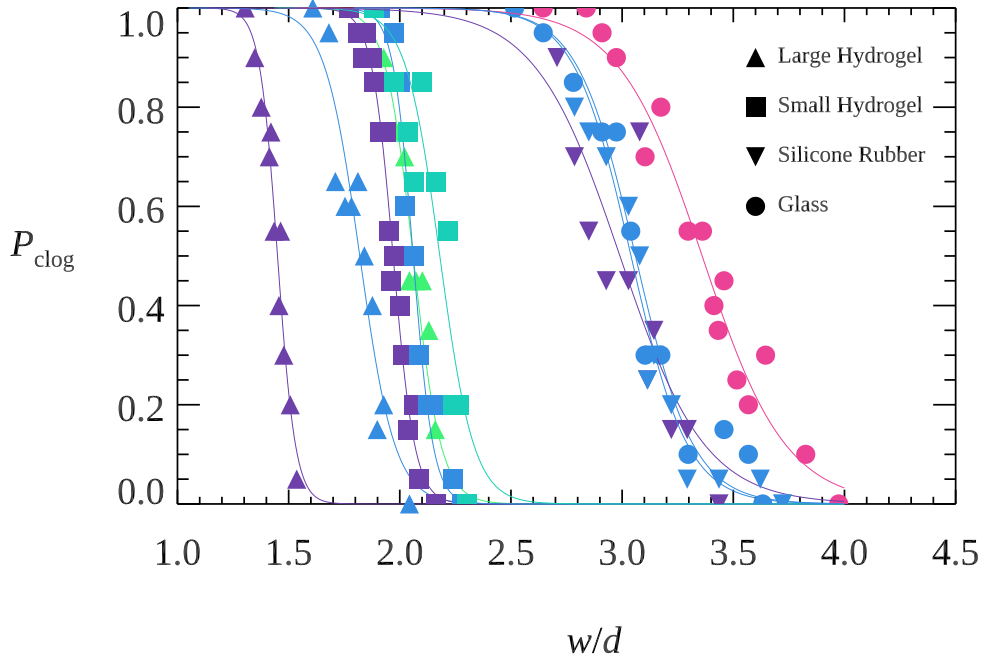


FIG. 3: Experimental probability of clogging as a function of w/d , the ratio of the hopper exit width w to the particle diameter d . Data for different types of particles with the influence of gravity varied by setting different tilt angles. Different symbols represent different types of particles as indicated in the legend. The different colors stand for different tilt angles θ : 90° (dark purple, largest influence of gravity), 50° (dark blue), 35° (light blue), 20° (green), and 10° (red, smallest influence of gravity). The lines are sigmoidal fits: $P_{\text{clog}}(w/d) = 1 + \exp[(w/d - a)/s]^{-1}$.

In Fig. 3 each family of symbol type indicates one type of particles. The influence of gravity is apparent: clogging is easier for reduced gravity, as signified by the curves shifting to the right in Fig. 3 as the colors vary from dark purple (maximal gravity) to blue to red (minimal gravity). For large hydrogel particles, as gravity decreases by a factor of 3, the location where $P_{\text{clog}} = 1/2$ shifts from $w/d \approx 1.4$ to 2.1. Different types of particles behave differently in the clogging experiment: harder particles are more likely to clog, also signified by the curves shifting to the right. With a tilt angle $\theta = 50^\circ$, the large hydrogel particles have $P_{\text{clog}} \approx 1/2$ at $w/d \approx 1.8$, the small hydrogel particles have $P_{\text{clog}} \approx 1/2$ at $w/d \approx 2.1$, and both the silicone rubber particles and glass particles have $P_{\text{clog}} \approx 1/2$ at $w/d \approx 3.1$.

Figure 4(a) shows a similar trend from the simulation data. As gravity is decreased, the particles effectively become harder, and clogging becomes easier; $P_{\text{clog}} = 1/2$ moves to larger values of w/d . A different view of simulation data telling the same story is shown in Fig. 5(a), where now the symbols correspond to fixed values of w/d and P_{clog} decreases as g is increased. Narrower hoppers (smaller w/d) are easier to clog and thus require higher values of g to reduce P_{clog} .

I wish to quantify and compare the different data sets to understand the influence of particle softness on clogging. Following Ref. [19], I fit the $P_{\text{clog}}(w/d)$ curves to sigmoidal fits of Fig. 3 and extract the opening width w/d for which $P_{\text{clog}} = 1/2$; this characterizes the ability of the system to clog. To quantify softness, I use the magnitude of deformation δ a particle has due to its weight, nondimensionalized by the particle diameter d . The experimental deformation δ is determined by balancing the weight of one particle with the Hertz contact force law, using the modulus data in Table I. For the simulation data, balancing the gravitational force on a particle with the contact force against a hypothetical horizontal wall leads to $\delta/d = 2g/F_0$.

Figure 6(a) shows that the parameter δ/d works fairly well to collapse all of our $w/d(P_{\text{clog}} = 1/2)$ data, including the laboratory data with hydrogel particles from our group's prior work [19]. The addition of the glass data extends the dynamic range of δ/d by two orders of magnitude over the prior work. Considering the differences between the simulation and the experiment, the experimental results are in great agreement with the simulation results suggesting that δ/d is a good measurement of the importance of softness. As δ/d gets larger (particles become softer), the hopper opening width needs to become smaller to have a 0.5 clogging probability. The one unexpected result is that the glass

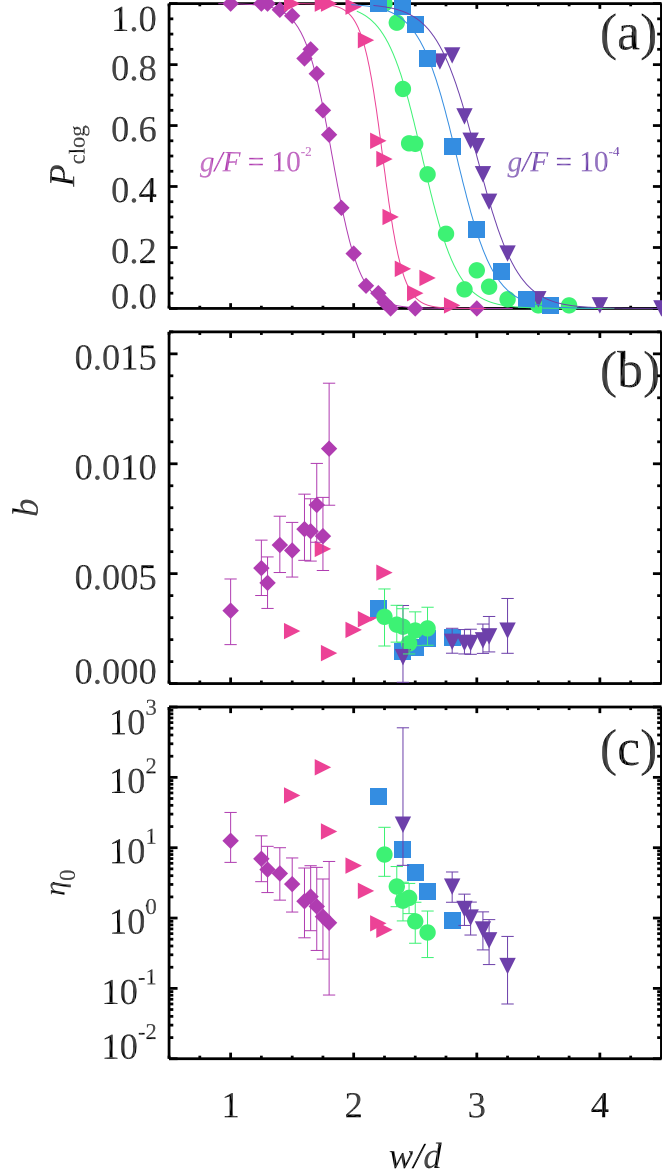


FIG. 4: (a) Clogging probability from the simulation, as a function of w/d , for fixed values of the driving force g . From left to right, $g/F_0 = 10^{-2}, 3 \cdot 10^{-3}, 10^{-3}, 3 \cdot 10^{-4}, 10^{-4}$. The lines are sigmoid fits. (b) Gompertz distribution fitting parameter b . (c) Gompertz distribution fitting parameter η_0 . For (b) and (c), representative error bars are drawn for three of the data sets, and represent 90% confidence intervals. The symbols are the same in all panels.

spheres, while being significantly harder and thus at much smaller values of δ/d , still show some dependence on δ/d . This may be indicating other effects not accounted for in δ/d such as frictional effects against the wall, which would depend on the experimental tilt angle θ .

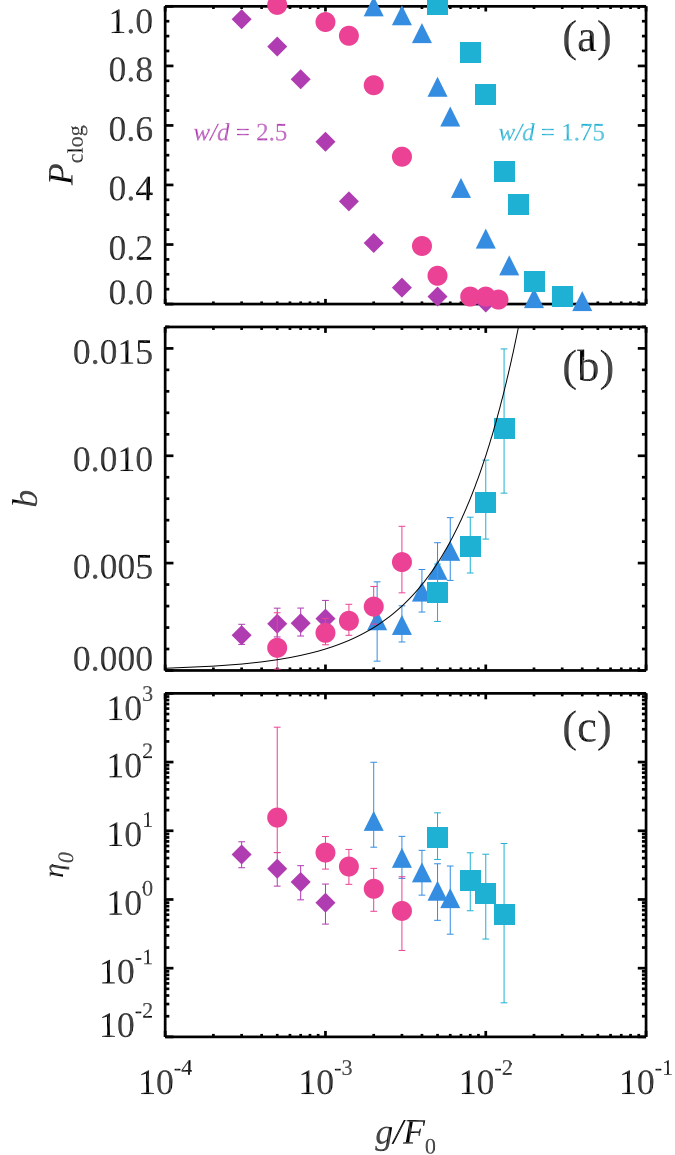


FIG. 5: (a) Clogging probability from the simulation, as a function of g/F_0 , for fixed values of the opening width w/d . From left to right, $w/d = 2.50, 2.25, 2.00$, and 1.75 . (b) Gompertz distribution fitting parameter b . The black line is the curve $b = g$. (c) Gompertz distribution fitting parameter η_0 . The error bars represent 90% confidence intervals.

Note that there is an important difference between the experiments and simulations: the experiments use 200 particles, whereas the simulations use 800 particles. More particles gives more chances to clog [27–30]. This difference between experiment and simulation could raise the experimental points to slightly higher values of w/d in Fig. 6(a).

Figure 6(b) shows the width of the sigmoidal fit s as a function of δ/d ; here the data do

not collapse, although they are of somewhat similar magnitude. Smaller values of s indicate stronger dependence of P_{clog} on w/d . For example, to change P_{clog} from 0.88 to 0.12, w/d needs to increase by $4s$, at least according to the sigmoidal fit. It is intriguing that all three hydrogel data sets have similar values of s , suggesting that the particle type is more influential than δ/d when it comes to determining s .

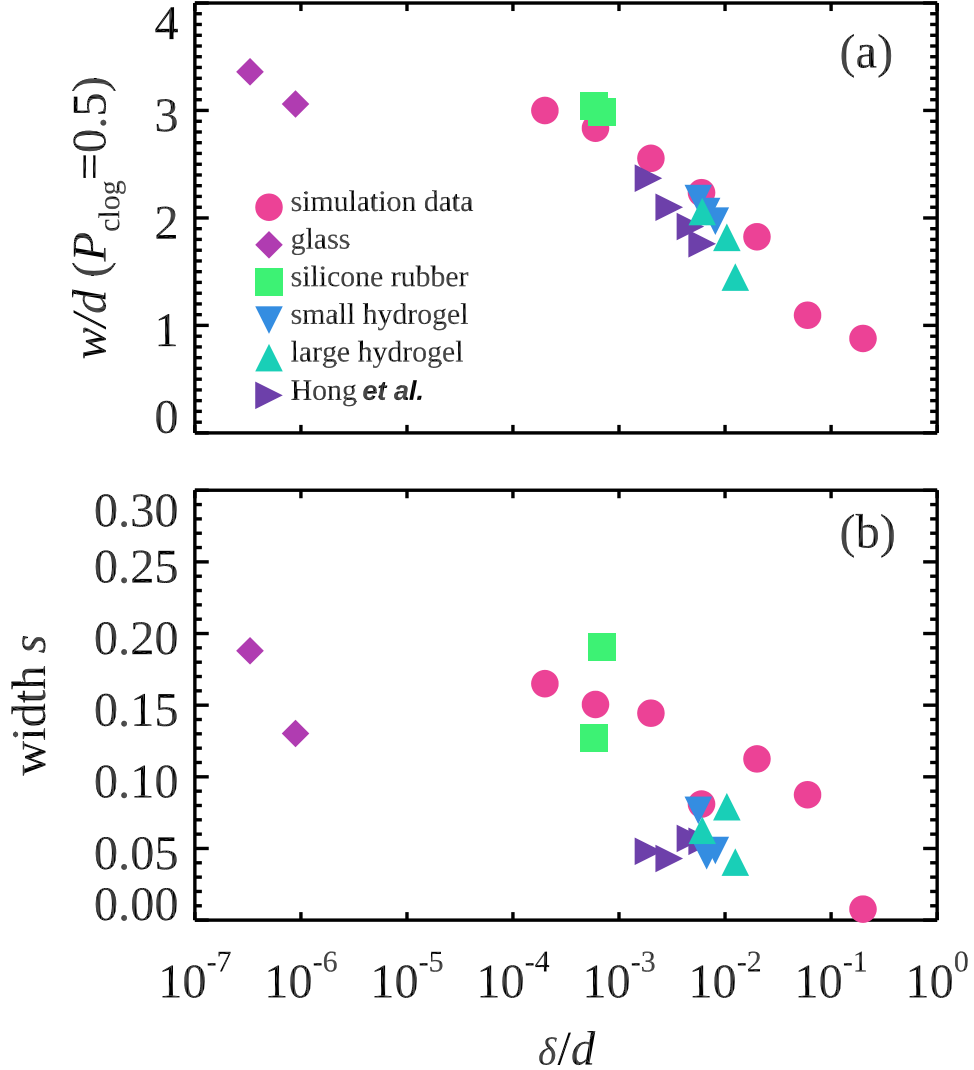


FIG. 6: Sigmoidal fit parameters. (a) Centers of sigmoidal fits for different types of particles under varying gravity, with the symbols corresponding to distinct experiments or simulations as indicated in the legend. (b) Width s of sigmoidal fits. The Hong *et al.* data are from Ref. [19] and are from a different set of hydrogel particles.

B. Number of particles remaining in hopper

I wish to understand how many particles remain in the hopper when it clogs. A simple hypothesis is that for soft particles, the weight of the particles above a clogging arch matters. If many particles are still in the hopper, then the arch must bear their weight – especially in the simulation for which there is no Janssen effect [31]. The Janssen effect is a reduction of pressure at the bottom of a container of particles due to friction [8, 32], and our simulations do not have friction. Likewise, recent experiments studying hydrogel particles measured the pressure at the bottom of the hopper and confirmed it depended on how many particles were in the hopper [22]. Thus, I hypothesize that clogging should be less likely when the hopper is full of particles, and more likely when the hopper has fewer particles. This is confirmed by the data, shown in Fig. 7(a). Here I measure the probability of a clog during the next 50 particles flowing out of the hopper, conditional on not having yet clogged. For example, all the simulations start with $N = 800$ particles. For Fig. 7(a) at $N = 600$, I am considering all the simulations which did not clog with more than 600 particles, and asking what is the probability that this subset of simulations has a clogging event before reaching $N = 550$ particles in the hopper. This probability rises as the hopper drains (as N decreases), confirming the hypothesis. The different data sets correspond to different values of w/d , with clogging probability larger for the data with smaller w/d . To measure the small probabilities, each data set in Fig. 7(a) is based on more than 1000 simulations.

The probability measured in Fig. 7(a) is related to the “hazard rate,” the rate of clogging events expected per unit particle exiting the hopper. Note that unlike probability, the hazard rate is indeed a rate and can be above 1, indicating an extreme likelihood of observing a clog, albeit with a small nonzero chance of not observing a clog. In contrast, I am focusing on the measured probability, bounded by 1, which behaves conceptually like the hazard rate when $P \ll 1$. Figure 7(a) is a semilog plot showing that the hazard rate rises exponentially as the hopper drains. This suggests that the probability distribution of N , the number of particles left in the hopper when it clogs, should follow the Gompertz distribution: the probability distribution corresponding to an exponentially growing hazard rate. The Gompertz distribution is often used to describe the lifespans of human beings and have wide application in actuarial science. The Gompertz distribution is not based on any clogging physics, and we treat it as a mathematical fitting function that works well for the

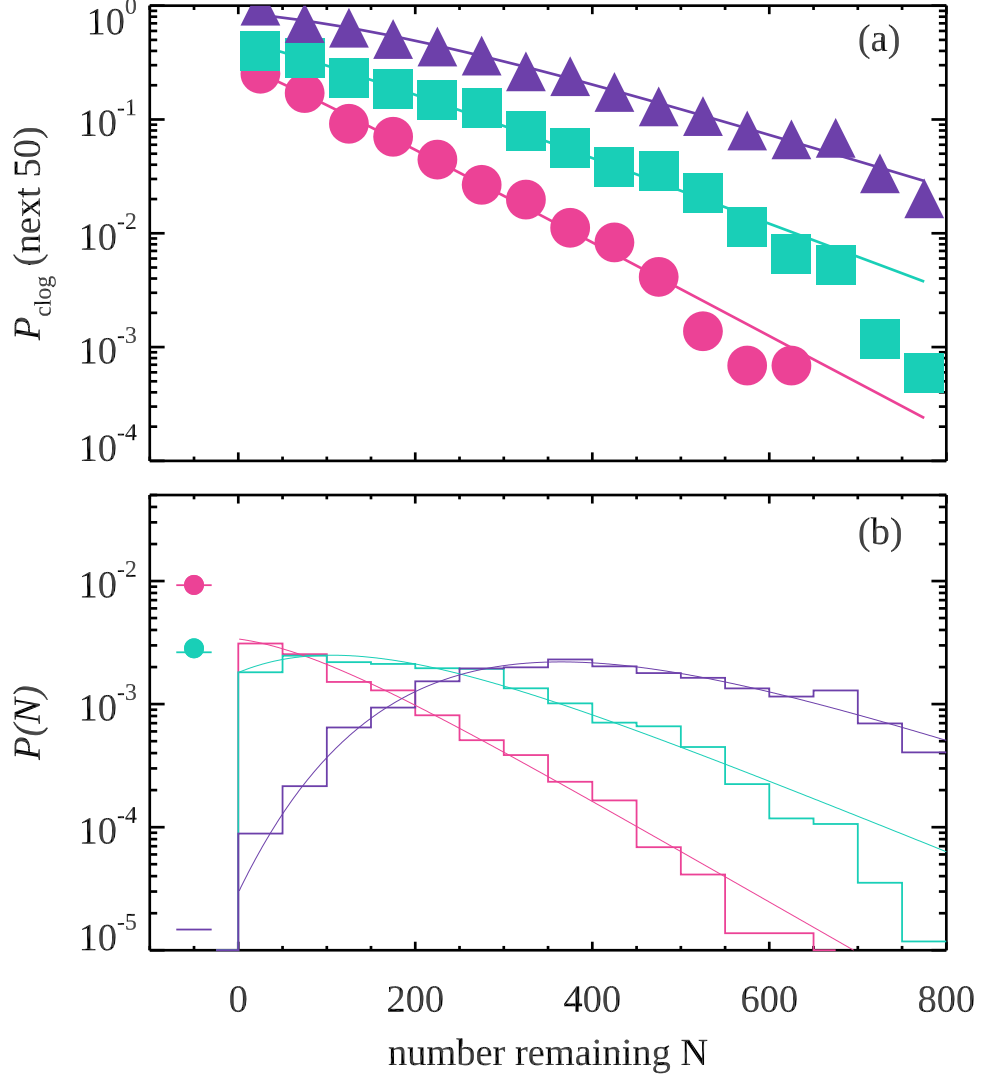


FIG. 7: (a) Hazard rate: probability of clogging as the next 50 particles flow out, as a function of the number of particles N left in the hopper. The lines are the best fit to the Gompertz hazard rate (integrated over the next 50 particles). From left to right, $w/d = 1.8, 1.6$, and 1.25 ; the data are taken from simulation runs with 1454, 1697, and 1579 trials respectively. For these data $g = 10^{-2}$. (b) Probability of clogging with N particles left in the hopper. The lines are the best fit to the Gompertz distribution. The circles at the left side of the plot indicate the probability the system does not clog (divided by 50 for comparison to the probability distribution); note that the $w/d = 1.25$ data always clogs in the simulation (for 1579 runs). The horizontal segments for $N < 0$ indicate the expected probability that the system does not clog, based on the Gompertz distribution.

simulation data and some of experimental data. In particular, consider $n = 800 - N$: the number of particles that have flowed out. If the hazard rate is given by $h(n) = \eta \exp(bn)$ then $P(n)$ is given by

$$P(n) = b\eta \exp(\eta + bn) \exp(-\eta e^{bn}). \quad (3)$$

To make more physical sense of the fitting parameters, I recast this in terms of N such that the hazard rate is

$$h(N) = \eta_0 \exp(-bN), \quad (4)$$

where now η_0 has the meaning of the hazard rate as $N \rightarrow 0$ (as the hopper empties). The parameter b expresses the rapidity of the growth of the hazard rate as the hopper drains. Figure 7(b) shows the measured probability distribution functions $P(N)$ for the number of particles left in the hopper, and the curved lines show the Gompertz distribution fits to the data (using maximum likelihood) [33]. The excellent agreement shows that the data are well described by the Gompertz distribution. The Gompertz distribution fit also predicts the probability that the system does not clog (in other words, the integral of Eqn. 3 from $n = 800$ to $n = \infty$). In fact, the observed probability of not clogging is information used to fit the Gompertz distribution. The circles at the left side of Fig. 7(b) indicate the observed clogging probability, and the horizontal line segments intersecting the circles show the predicted clogging probability from the Gompertz distribution fit. Likewise, the probability of clogging during the next 50 particles exiting shown in Fig. 7(a) (symbols) is well-fit by the prediction of this quantity from the Gompertz distribution fit (lines).

The influence of w/d and g can be understood by the Gompertz fitting parameters b and η_0 , shown in Fig. 4(b,c) respectively. b stays fairly small, $O(10^{-3} - 10^{-2})$, consistent with needing $O(10^2 - 10^3)$ particles to flow out for significant increases in the hazard rate. η_0 decreases dramatically as w/d increases, indicating that the system becomes increasingly unlikely to clog even as $N \rightarrow 0$. In contrast, as w/d is decreased, η_0 rises to well above 1, reflecting the observation that not only do I always see clogging in the simulation, but that it always is observed to clog with many particles still remaining in the hopper – which is illustrated by the $w/d = 1.25$ data in purple in Fig. 7(b) for which the system did not empty out for any of the 1579 simulation runs. Note that the error bars in Fig. 4(b,c) are largest when $P_{\text{clog}} \rightarrow 1$ or $\rightarrow 0$, for which there's less variability in the observations of N and thus less constraints on the fitting.

A complementary view of the simulation data is given in Fig. 5, where each symbol type corresponds to a fixed value of w/d , and the horizontal axis shows the dependence on g (varying over three decades). Figure 5(a) shows the expected result, that at fixed w/d increasing g decreases clogging. If all that mattered for the hazard rate (at fixed w/d) is the weight of the pile above for a given N , then it would make sense that $b \sim g$, see Eqn. 4 where the weight is $\sim Ng$. The prediction $b = g$ is the black curve drawn in Fig. 5(b), showing this works reasonably well for all the data except the purple symbols ($w/d = 2.50$). Of course, this predicts that b is constant when considering data at constant g , which is somewhat true for the smallest values of g in Fig. 4(b) but clearly false for the largest value of g in that graph. The data of Fig. 5(c) shows that η_0 decreases as a power law with g , although not with a fixed exponent. Fitting $\eta_0 \sim g^{-\alpha}$, for $w/d = 2.50, 2.25, 2.00, 1.75$ the best fit power law exponent is $\alpha = -1.3, -1.7, -2.4, -2.7$.

The limit $g \rightarrow 0$ is important in that it represents perfectly hard particles [34]. Our group's prior work suggested that the data of Fig. 6(a) should reach an asymptote for small g , although as noted above the glass particles data suggest that there is still some additional dependence on the forcing, perhaps due to frictional effects. Thinking just of the simulation data, Fig. 5(b) suggests that if $b \sim g$, the hard particle limit is $b = 0$ signifying that the hazard rate is independent of the number of particles in the hopper. This certainly seems to be the case for the classic clogging of hard particles, for which the output flux is independent of the number of particles in the hopper [5, 10, 35]. For the fit parameter η_0 , assuming $b = 0$ for hard particles means that η_0 is the constant hazard rate for clogging, which should not depend on g for hard particles. This is for example consistent with an experiment that used a centrifuge to vary g , finding no dependence on g [36], although Ref. [19] pointed out that those particles were not infinitely hard but rather had $\delta/d \approx 10^{-6}$.

To compare to the experiment, when the experiment clogs I measure the number of particles remaining in the hopper. For the experiment, this is not an exact count but rather an approximation based on image analysis. Ideally I would wish to use image analysis to directly identify and count the particles. However, given that many of the experiments use soft particles which are deformed and closely touching, this sort of image analysis proved problematic. Instead, when the hopper clogs, I determine the boundary of the region of the image containing particles in the hopper, and then measure the area contained within that region. To calibrate this I took 10 photographs with exactly 200 particles in the hopper for

the same imaging conditions as the experiment (same particle type, same tilt angle, same lighting conditions) and measure the area those 200 particles occupy. This then gives us the mean area per particle. For the experimental data of interest, my uncertainty in number of particles remaining in the hopper is ± 10 from this method: as will be seen, the results do not depend sensitively on this uncertainty. I used this method to estimate the number N of particles left in the hopper when samples clogged, using 300 trials for three different particle types, and w/d such that $P_{\text{clog}} \approx 0.7$ so that a large number of clogging events would be observed.

The experimental data are plotted in Fig. 8, along with the best fit to the Gompertz distribution. The hydrogel data are reasonably well fit, but the silicone rubber and glass data both disagree with the fit. In particular, for a sample that does not clog 30% of the time, one expects that when clogging occurs, it should more often occur with fewer particles in the hopper. That is the argument given above for the simulation data, that when the hopper drains out the pressure decreases and thus it is easier to form an arch that can support the weight of the remaining particles. However, for the silicone rubber particles and the glass particles, it appears that it is most likely for the experiment to clog near the start of the experiment; and the more particles that have flowed out, the less likely it is to clog. I can speculate as to the causes. First, the silicone rubber particles have more friction, whereas the glass particles are significantly harder; both of these may frustrate the argument about pressure making a difference to the clogging arch formation. Second, the particles also are more massive, and it may be that as they fall through the hopper, they add extra vibrations to the apparatus. Vibrations are well-known to destabilize clogging arches [12]. Perhaps it is easier for an arch to form before the apparatus starts shaking too much, and harder after particles are flowing out in significant quantity. In any case, I note that by comparison the hydrogel data agree reasonably well with the Gompertz distribution fit. It is further interesting to note that despite the disagreement with the Gompertz distribution fit, nonetheless the silicone rubber and glass particles fit well on my clogging plot in Fig. 6(a); and the glass particle arch size data also agrees well with the hydrogel and simulation data in Fig. 9(b), as well be discussed in the next section.

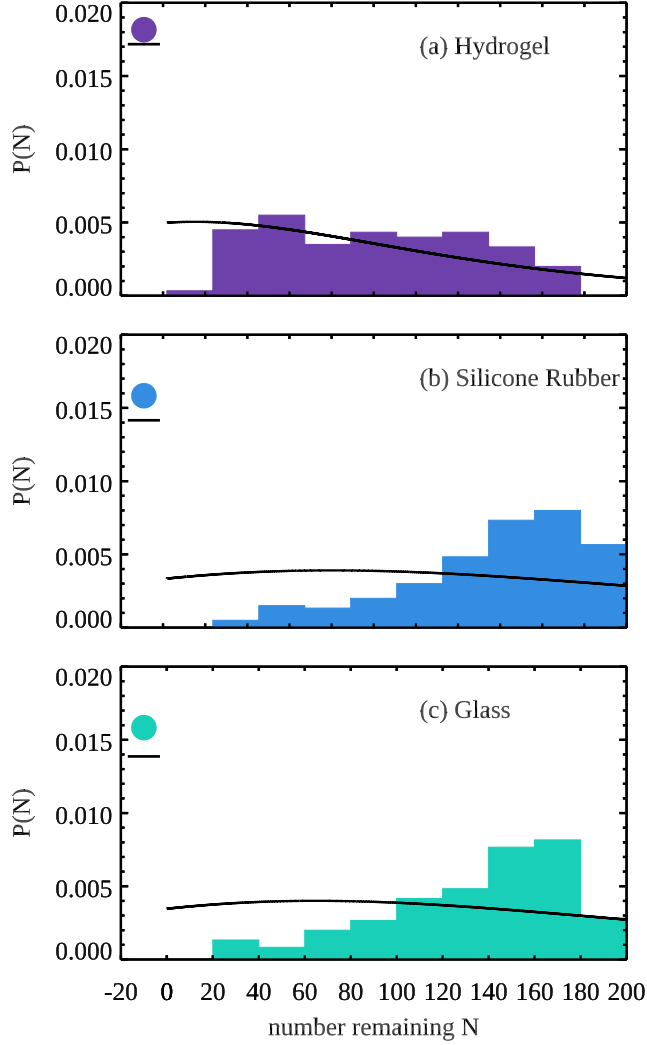


FIG. 8: Histograms of probability of clogging with N particles left in the hopper for (a) hydrogel particles, (b) silicone rubber particles, and (c) glass particles with $\theta = 50^\circ$. The solid black lines are the best fit to the Gompertz distribution. The circles at the left side of the plot indicate the probability the system does not clog (divided by 20 for comparison to the probability distribution). The horizontal segments for $N < 0$ indicate the expected probability that the system does not clog, based on the Gompertz distribution.

C. Arch size

When the clogging happens, I count the number of particles forming the arch. The simulation results are shown in Fig 9(a); different symbols and colors indicate different values of the gravitational driving g . The excellent collapse of the data shows that the average arch

size solely depends on the exit width w/d independent of the magnitude of g . The smallest arch has one particle, and this is only seen for small values of $w/d < 1.0$. As w/d increases to 1.5, the average arch size increases to three. There is a plateau for $1.5 \lesssim w/d \lesssim 2.3$ where the average arch size is constant at 3. This plateau was also seen in prior experimental data with hard particles [37], although in that work it was more pronounced when the hopper wedge angle was larger than my moderate 34° angle. At higher values of w/d there is a smaller plateau with arch size equal to 4, and then a bit of data with the mean arch size rising to 5 at the lowest value of g ($g = 10^{-4}$) and $w/d \gtrsim 3.5$.

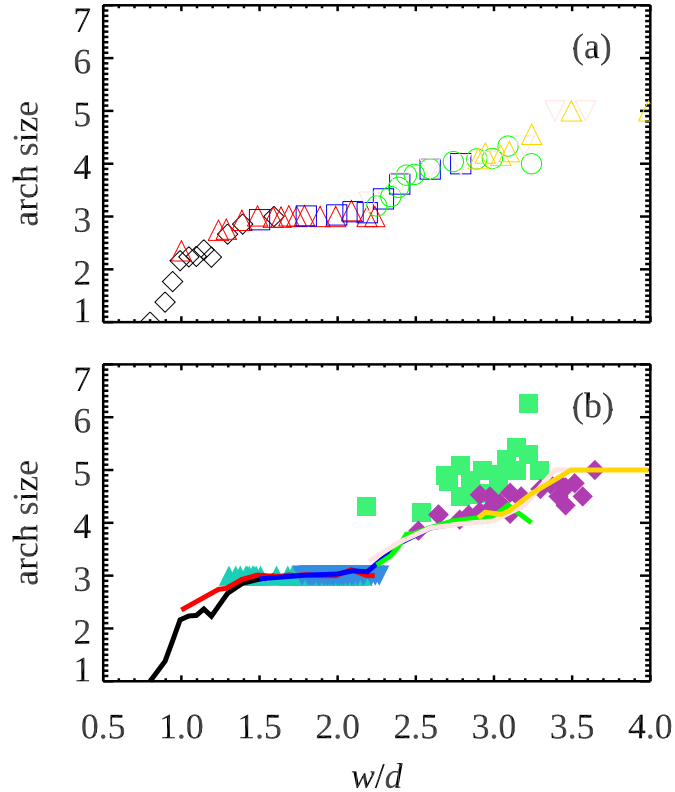


FIG. 9: Average arch size as a function of w/d , the ratio of the hopper exit width w to the particle diameter d . (a) Data from the simulation. Different values of gravitational driving are indicated by the different symbols and colors; from left to right, $g = 0.03, 0.01, 0.003, 0.001, 0.0003$, and 0.0001 . (b) The lines reprise the simulation data from (a). The symbols are the experimental data using different types of particles under the influence of different values of gravity. The symbols are the same as Fig. 6; in particular, the green squares that are outliers correspond to the silicone rubber particles, which have a significantly higher coefficient of static friction.

To compare the experiment and simulation, the simulation data are replotted in Fig. 9(b) as the lines, with the same colors as in panel (a). The experimental results are plotted with symbols [corresponding to the legend in Fig. 6(a)]. The experimental results for the hydrogel particles and glass particles agree with the simulation result supporting that the arch size is affected by the opening width and is independent of the magnitude of gravity. This strongly suggests for these particles – ranging from quite soft to quite hard, more than 5 orders of magnitude in δ/d – the clogging arch is solely determined by geometry. In contrast, the results for silicone rubber particles deviate significantly from the other results: For a given opening width, the average arch size will be larger than that for simulation and the glass particles. I attribute the difference between the silicone rubber particles and the other data to be due to the silicone rubber particles' large coefficient of sliding friction. The sliding friction for silicone rubber particles is 0.4 ± 0.2 , while the sliding friction for glass marble particles is 0.009 ± 0.002 , and the simulation has no friction. Indeed, the arch shown in Fig. 1(d) has one particle that is clearly held in place by friction. While this is an uncommon result, this obvious frictional effect is observed several times in my experiments with the silicone rubber particles (and never with any other particles).

D. Flux Law

After having a good understanding of the clogging process of soft particles, I am interested in describing how the flow rate is influenced by the opening exit width and gravitational condition. The flow rate is determined by the pressure near the exit width, which is caused by the weight of particles above the hopper. Due to the ineffectiveness of the Janssen effect for soft and frictionless particles, the pressure near the exit should be hydrostatic pressure $P = \rho gy$, where ρ is the density of soft particles, and y is the depth (the maximum height of particles in the hopper) [20]. In the simulation, as the hopper has two vertical sidewalls restraining soft particles, the maximum height of particles in the hopper is linearly related to the number of particles remaining in the hopper. As a result, I try to find the relationship between the flux and number of particles remaining in the hopper. With data from 10 simulations for chosen exit width and gravity, I can get the average of flux as a function of the number of particles remaining in the hopper. As the hopper drains (as N decreases), the flux will decrease. I find a strong linear relationship between the flux and number of

particles remaining in the hopper. I fit simulation results linearly as shown in Fig. 10.

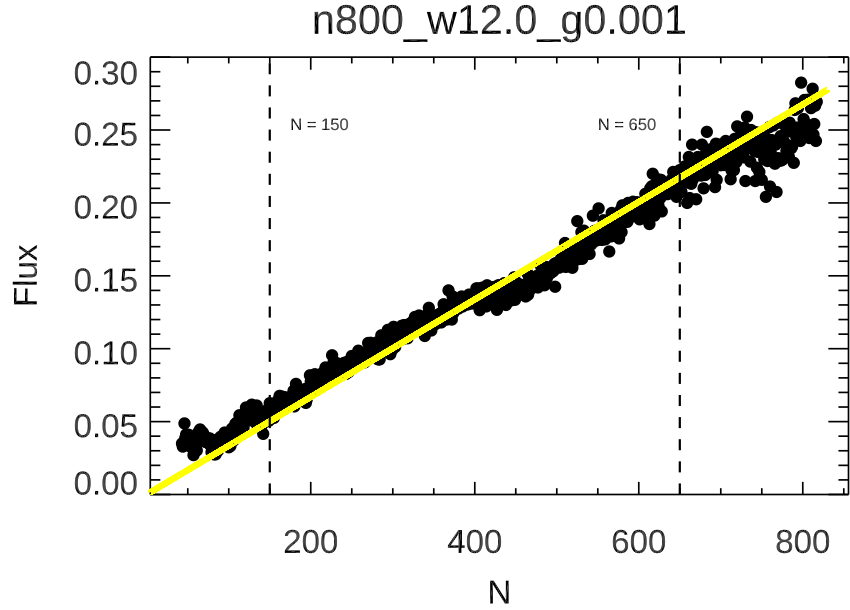


FIG. 10: Simulation data of the flux and number of particles remaining in the hopper. The yellow solid line is the linear fitting line where I fit in the range $150 \leq N \leq 650$.

There are long transition states at the beginning and near the end of simulation as shown in Fig. 15 (c). At the beginning of the simulation when particles start to flow out of the hopper, it takes some time for them to accelerate and reach steady states; near the end of the simulation, there are too few particles left in the hopper. Transitions result in non-linear situations so that I only fit data in stable areas. I set two cutoff points at $N = 150$ and $N = 650$ and I try to cover as much linear regions as possible. I start fitting when there are 650 particles left in the hopper and the fitting ends when there are less than 150 particles left in the hopper. Most simulations reach steady state in this region. Fitting lines pass through the origin because the flux will spontaneously become 0 when there is no particle left in the hopper.

Then the flux is:

$$\Phi = C \times N \quad (5)$$

C is the parameter of the linear fittings (the slope) and I investigate how it is determined by the gravitational condition g and exit opening width w . I run simulations with a wide

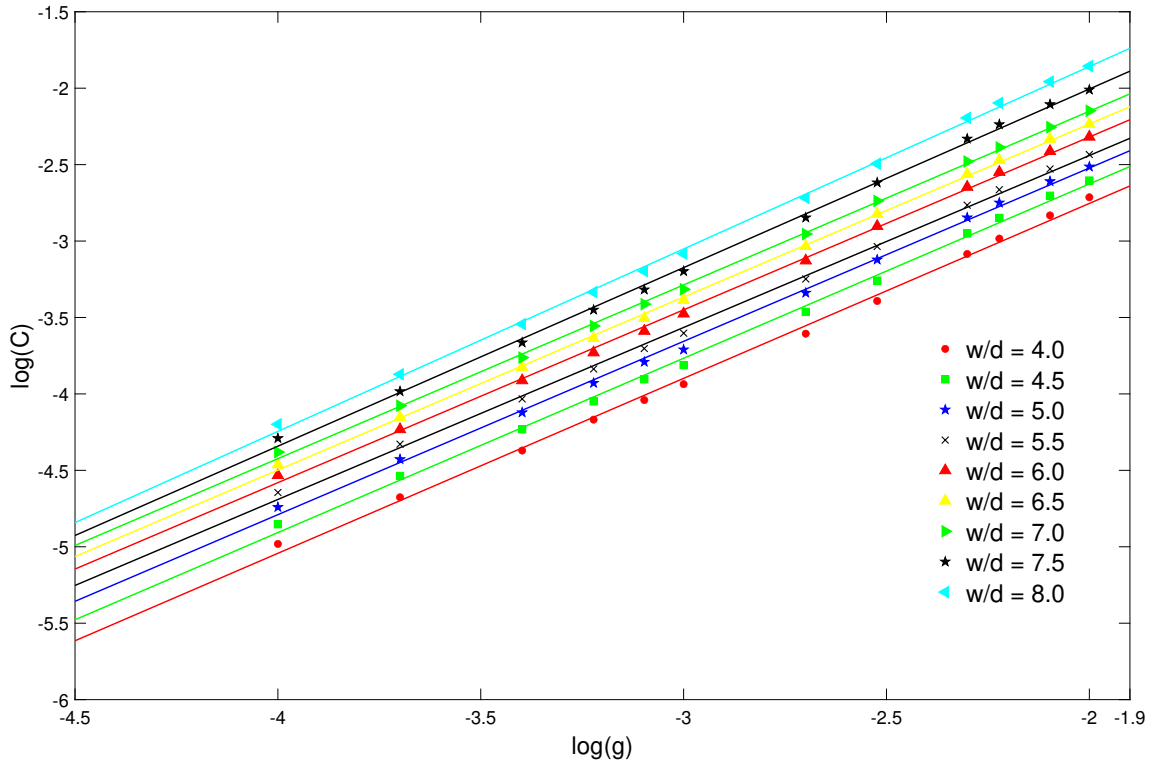


FIG. 11: Plot of C and g in log-log scale. Different symbols represent simulation data with various w/d . Solid lines are linear fittings. A strong linear relationship in log-log plot suggests a power law.

range of gravity driving $10^{-4} \leq g \leq 10^{-2}$ and various opening exit width $8 \leq w \leq 16$ which could give us a general conclusion for the outflow of soft particles under different conditions. I find that when the gravity driving is too large ($g \geq 0.1$), particles are over-compressed and flow out of the hopper like fluid. When I plot C and the gravity driving g in a log-log scale, the linear fitting lines suggest a power law between C and gravity g as shown in Fig. 11. C can be written in the form:

$$C = \alpha \times g^a \quad (6)$$

a is the slope of the line in Fig. 11 and alpha is ten to the power of the interception. Both are determined by the ratio between the exit width and particle's diameter. For small values of w/d , α holds constant and a increases linear with w/d as shown in Fig. 12. I only

fit parameters for $4 \leq w/d \leq 6.5$, I can recast the expression for flux as:

$$\Phi = 0.286 \times \left(\frac{w}{d} - 2.95\right) \times g^{1.13} \times N \quad (7)$$

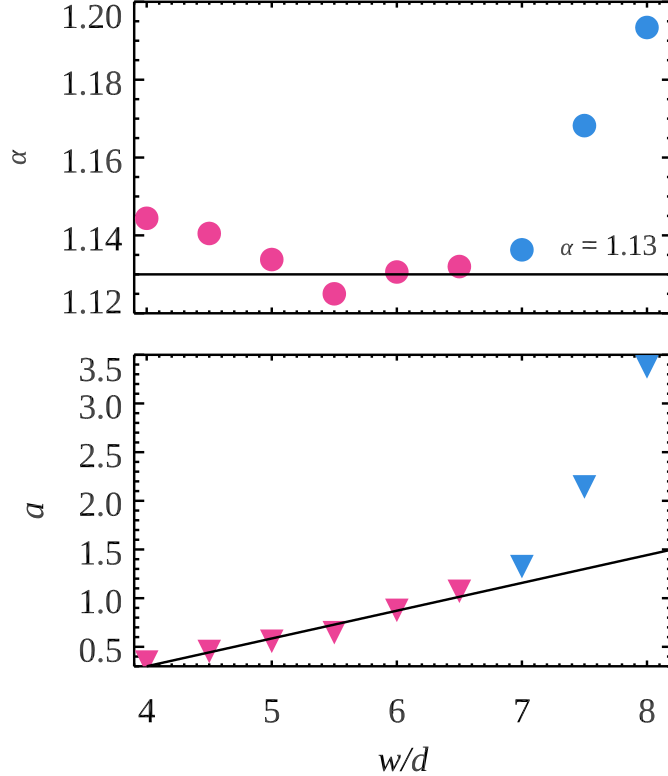
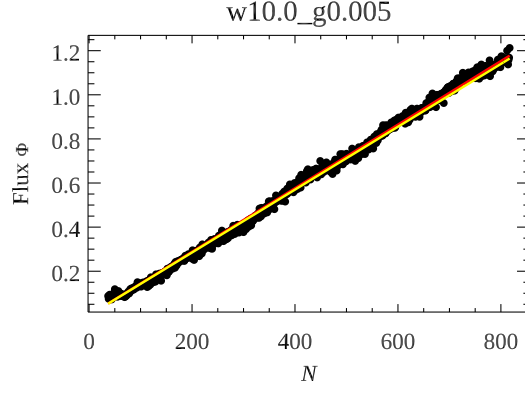
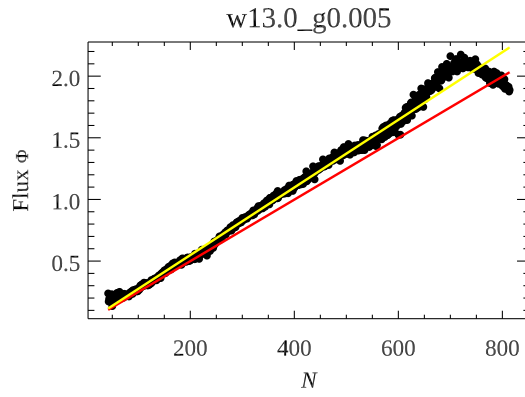


FIG. 12: Plot of α and a as a function of w/d . Circles are data for α and downward triangles are data for a . Red symbols represent data involved in fitting and blue symbols are data that are ignored when I fit the flux law. I find that for small w/d , α is almost a constant, and a increases linearly with w/d .

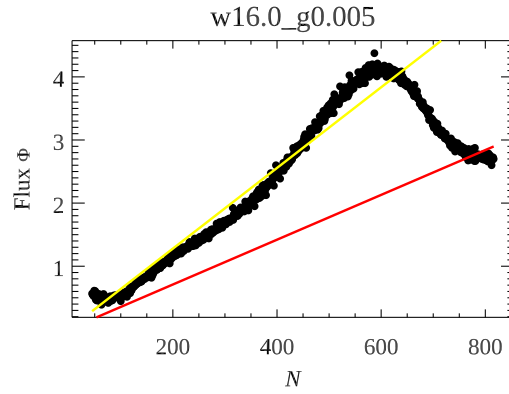
I compare the flux law with simulation results in Fig. 13. As expected, the flux law can describe the outflow of soft particles with relatively small opening exit widths. The flux law deviates from simulation data when the exit width is too large. This result suggests that some geometry properties of the hopper are missing when the exit width is too large so that particles flow out of the hopper much faster than what I can induce from small w/d data. The distance between two vertical walls in the simulation is 20 so that when the opening exit is large, slides of the hopper become very small and can not hinder the outflow of soft particles effectively. Most particles will just flow out of the hopper without colliding with slides or adjacent particles. Hence, the flux predicted from the flux law is much smaller than



(a)



(b)



(c)

FIG. 13: Plots of simulation data, linear fitting and the flux law for $g = 0.005$. Black circles are simulation results. Yellow solid lines are linear fitting of simulations. Red solid lines are flux according to the flux law (Eqn. 7). (a) The flux law perfectly describes the flux for simulation with $w = 10$. (b) Results for $w = 13$. (c) The flux law fails for simulation with $w = 16$ and a huge curvature occurs when $N \approx 600$.

simulation results for large exit width. Further studies are required to include the change of hopper geometry into the flux law.

I notice that for large gravity driving ($g > 0.003$) and large exit widths, there is a curvature at the beginning of the simulation. I investigate the particles' average velocity along the vertical direction and density in the hopper. Curvature is mainly due to non-uniform behavior of average velocity in the y direction and the density. When average velocity in y and density change uniformly with the number of particles left in the hopper or the y position, simulation data form a perfect linear line as shown in Fig. 14.

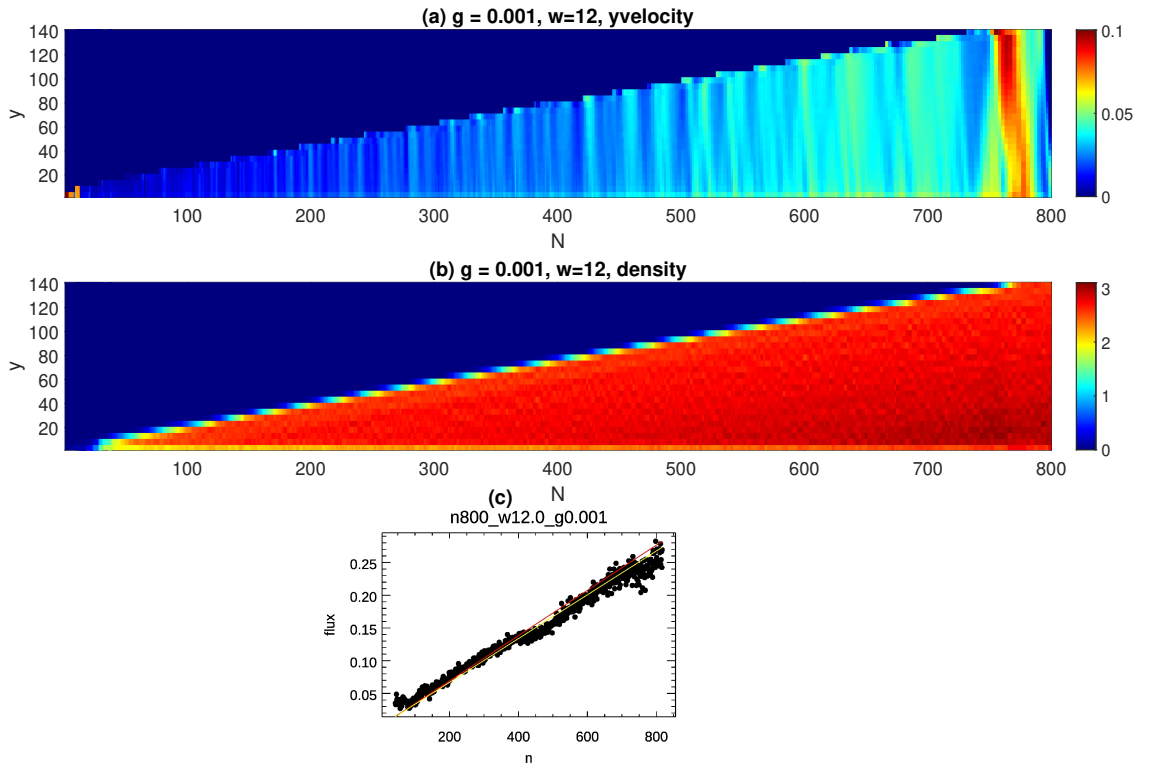


FIG. 14: Average velocity in the y direction and density of ten simulations for $g = 0.001$ and $w = 12$. (a) Velocity in the y direction for corresponding number of particles left in the hopper N and height y . (b) Density in the hopper. (c) Simulation data. There is a linear relationship between the flux Φ and number of particles in the hopper N .

When particles near the bottom are too relaxed as shown in Fig. 15 at the beginning of the simulation, particles on top will accelerate and result in a curvature. It is not completely clear why this curvature occurs but it suggests that simulations with large gravity driven g

and large exit width w take longer to reach steady states.

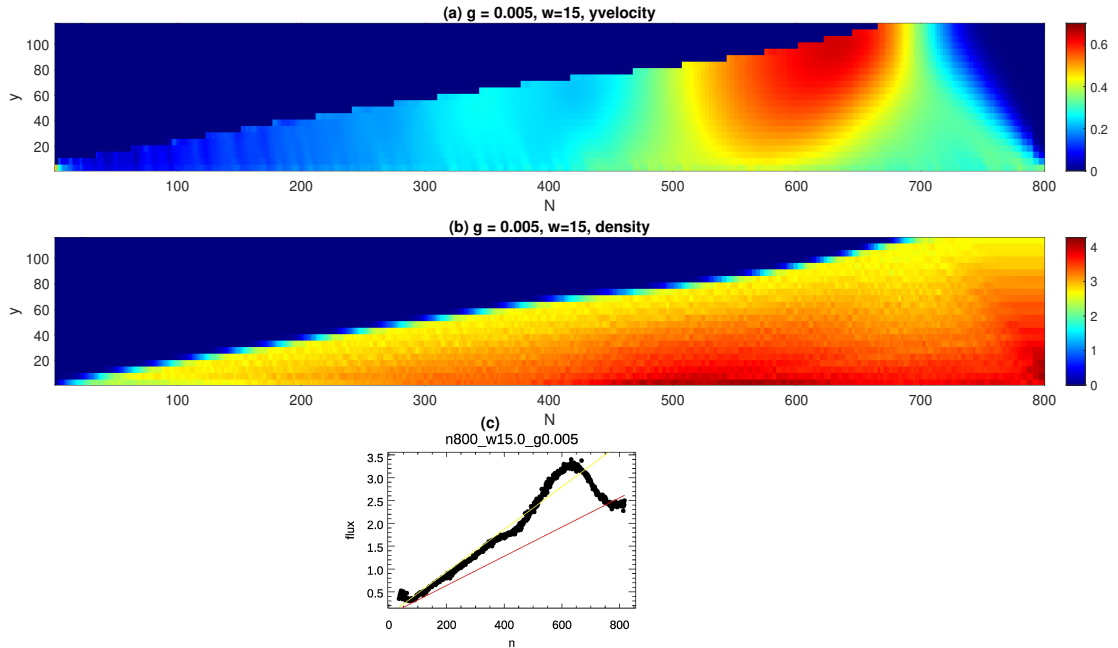


FIG. 15: Average velocity in the y direction and density of ten simulations for $g = 0.005$ and $w = 15$. (a) Velocity in the y direction for corresponding number of particles left in the hopper N and height y . (b) Density in the hopper. (c) Simulation data. There is a linear relationship between the flux Φ and number of particles in the hopper N .

V. CONCLUSIONS

Work in recent years has shown that the clogging of soft particles is qualitatively different than hard particles [13, 19–22]. I extend this prior work with two new types of particles, silicone rubber and glass, showing that there is a relatively continuous transition from the softest particles to the hardest [Fig. 6(a)]. The agreement between hydrogel data, rubber data, glass data, and simulation data – with no free fitting parameters – is strong evidence for universal behavior of soft particle clogging. This is further supported by examining the mean arch size, which is a function of only w/d (exit opening width w divided by the particle diameter d). The caveats are that this is not true for the rubber particles for which friction is nearly two orders of magnitude higher; and the mean arch size is also known to depend

on the hopper wedge angles [37]. My final analysis considers the number of particles left in the hopper, further finding a difference between the rubber and glass particles, as compared to the simulation and hydrogel particles. For rubber and glass particles, if they clog, it is slightly more likely to do so near the start of the experiment. In contrast, for the hydrogel and simulated particles, they are likelier to clog near the end of the experiment, strong evidence that the hydrostatic pressure of the particles in the hopper [22] breaks arches and prevents clogging.

My work shows that for soft hydrogel particles and simulated soft particles, the number of particles left in the hopper when a clog occurs is well fit by the Gompertz distribution. This distribution applies when the clogging “hazard rate” rises exponentially as the hopper drains. The direct implication of this is that the hydrostatic pressure of the soft particles influences clogging; that it is harder to form a clogging arch with many particles in the hopper as the hydrostatic pressure causes the soft particles in the arch to deform and break the arch. A subtler implication of the Gompertz distribution fit is that there is some chance of the hopper clogging even when the hopper is full of particles; albeit that the chance is exponentially small. This further suggests that even with large hopper openings w/d there is still some chance of clogging, consistent with prior observations of clogging that suggested that there is no critical exit size for causing clogging; rather, clogging becomes exponentially unlikely as the opening size is increased [27, 28, 35]. Finally, the Gompertz distribution fit also implies that in the opposite limit of a small opening size, there may nonetheless be some finite probability that the hopper does *not* clog. It seems plausible that there is some limit on this, that for opening widths smaller than the particle size and sufficiently stiff particles, the system will always clog. Nonetheless, the results imply that the ability to completely flow out may persist to surprisingly narrow exit openings, even if the chance to not clog becomes exponentially rare.

Through simulations, I derive a flux law to describe how fast soft particles flow out of the hopper with varying opening exit widths under different gravitational conditions. For small values of exit widths, the flux predicted matches with simulation data. However, when the exit width is too large, simulation result is much greater than what I can get from the flux law. This deviation between the flux law and simulation data at large exit widths suggests

that some geometry properties of the hopper diminish when I have a very large exit width.

- [1] W. E. Deming and A. L. Mehring, The gravitational flow of fertilizers and other comminuted solids, *Ind. Eng. Chem.*, **21**, 661–665 (1929).
- [2] F. C. Franklin and L. N. Johanson, Flow of granular material through a circular orifice, *Chem. Eng. Sci.*, **4**, 119–129 (1955).
- [3] R. L. Brown and J. C. Richards, Two- and Three-Dimensional flow of grains through apertures, *Nature*, **182**, 600–601 (1958).
- [4] R. T. Fowler and J. R. Glastonbury, The flow of granular solids through orifices, *Chem. Eng. Sci.*, **10**, 150–156 (1959).
- [5] W. A. Beverloo, H. A. Leniger, and J. van de Velde, The flow of granular solids through orifices, *Chem. Eng. Sci.*, **15**, 260–269 (1961).
- [6] A. W. Jenike, Quantitative design of mass-flow bins, *Powder Tech.*, **1**, 237–244 (1967).
- [7] K. To, P. Y. Lai, and H. K. Pak, Jamming of granular flow in a two-dimensional hopper, *Phys. Rev. Lett.*, **86**, 71–74 (2001).
- [8] R. M. Nedderman, U. Tuzun, S. B. Savage, and G. T. Houlsby, The flow of granular materials—I : Discharge rates from hoppers, *Chem. Eng. Sci.*, **37**, 1597–1609 (1982).
- [9] H. Sheldon and D. Durian, Granular discharge and clogging for tilted hoppers, *Granular Matter*, **12**, 579–585 (2010).
- [10] M. A. Aguirre, J. G. Grande, A. Calvo, L. A. Pugnali, and J. C. Géminard, Pressure independence of granular flow through an aperture, *Phys. Rev. Lett.*, **104**, 238002 (2010).
- [11] T. J. Wilson, C. R. Pfeifer, N. Mesyngier, and D. J. Durian, Granular discharge rate for submerged hoppers, *Papers in Physics*, **6**, 060009 (2014).
- [12] I. Zuriguel, D. R. Parisi, R. C. Hidalgo, C. Lozano, A. Janda, P. A. Gago, J. P. Peralta, L. M. Ferrer, L. A. Pugnali, E. Clément, D. Maza, I. Pagonabarraga, and A. Garcimartín, Clogging transition of many-particle systems flowing through bottlenecks, *Scientific Reports*, **4**, 7324 (2014).
- [13] K. Harth, J. Wang, T. Börzsönyi, and R. Stannarius, Intermittent flow and transient congestions of soft spheres passing narrow orifices, *Soft Matter*, **16**, 8013–8023 (2020).
- [14] D. Helbing, I. Farkas, and T. Vicsek, Simulating dynamical features of escape panic, *Nature*,

- 407**, 487–490 (2000).
- [15] A. Garcimartín, J. M. Pastor, C. Martín-Gómez, D. Parisi, and I. Zuriguel, Pedestrian collective motion in competitive room evacuation, *Scientific Reports*, **7** (2017).
 - [16] R. C. Hidalgo, D. R. Parisi, and I. Zuriguel, Simulating competitive egress of noncircular pedestrians, *Phys. Rev. E*, **95** (2017).
 - [17] Y. Bertho, C. Becco, and N. Vandewalle, Dense bubble flow in a silo: An unusual flow of a dispersed medium, *Phys. Rev. E*, **73**, 056309 (2006).
 - [18] G. Lumay, J. Schockmel, D. Henández-Enríquez, S. Dorbolo, N. Vandewalle, and F. Pacheco-Vázquez, Flow of magnetic repelling grains in a two-dimensional silo, *Papers in Physics*, **7**, 070013 (2015).
 - [19] X. Hong, M. Kohne, M. Morrell, H. Wang, and E. R. Weeks, Clogging of soft particles in two-dimensional hoppers, *Phys. Rev. E*, **96**, 062605 (2017).
 - [20] A. Ashour, T. Trittel, T. Börzsönyi, and R. Stannarius, Silo outflow of soft frictionless spheres, *Phys. Rev. Fluids*, **2** (2017).
 - [21] R. Stannarius, D. S. Martinez, T. Börzsönyi, M. Bieberle, F. Barthel, and U. Hampel, High-speed X-ray tomography of silo discharge, *New J. Phys.* (2019).
 - [22] T. Pongó, V. Stiga, J. Török, S. Lévy, B. Szabó, R. Stannarius, R. C. Hidalgo, and T. Börzsönyi, Flow in an hourglass: particle friction and stiffness matter, *New J. Phys.*, **23**, 023001 (2021).
 - [23] N. Bouklas and R. Huang, Swelling kinetics of polymer gels: comparison of linear and nonlinear theories, *Soft Matter*, **8**, 8194–8203 (2012).
 - [24] N. L. Cuccia, S. Pothineni, B. Wu, J. Méndez Harper, and J. C. Burton, Pore-size dependence and slow relaxation of hydrogel friction on smooth surfaces, *PNAS*, **117**, 11247–11256 (2020).
 - [25] D. J. Durian, Foam mechanics at the bubble scale, *Phys. Rev. Lett.*, **75**, 4780–4783 (1995).
 - [26] S. Tewari, D. Schiemann, D. J. Durian, C. M. Knobler, S. A. Langer, and A. J. Liu, Statistics of shear-induced rearrangements in a two-dimensional model foam, *Phys. Rev. E*, **60**, 4385–4396 (1999).
 - [27] K. To, Jamming transition in two-dimensional hoppers and silos, *Phys. Rev. E*, **71**, 060301 (2005).
 - [28] A. Janda, I. Zuriguel, A. Garcimartín, L. A. Pugnaloni, and D. Maza, Jamming and critical outlet size in the discharge of a two-dimensional silo, *Europhys. Lett.*, **84**, 44002 (2008).

- [29] J. Tang, S. Sagdiphour, and R. P. Behringer, Jamming and flow in 2D hoppers, *AIP Conf. Proc.*, **1145**, 515–518 (2009).
- [30] P. G. Lafond, M. W. Gilmer, C. A. Koh, E. D. Sloan, D. T. Wu, and A. K. Sum, Orifice jamming of fluid-driven granular flow, *Phys. Rev. E*, **87**, 042204 (2013).
- [31] H. A. Janssen, Versuche über Getreidedruck in Silozellen, *Zeitschr. d. Vereines deutscher Ingenieure*, **39**, 1045–1049 (1895).
- [32] J. H. Shaxby, J. C. Evans, and V. Jones, On the properties of powders. the variation of pressure with depth in columns of powders, *Trans. Faraday Soc.*, **19**, 60–72 (1923).
- [33] P. Nelson, *Physical Models of Living Systems* (W. H. Freeman, New York, NY), illustrated edition edition (2014), ISBN 978-1-4641-4029-7.
- [34] R. Arevalo and I. Zuriguel, Clogging of granular materials in silos: effect of gravity and outlet size, *Soft Matter*, **12**, 123–130 (2016).
- [35] C. C. Thomas and D. J. Durian, Fraction of clogging configurations sampled by granular hopper flow, *Phys. Rev. Lett.*, **114**, 178001 (2015).
- [36] S. Dorbolo, L. Maquet, M. Brandenbourger, F. Ludewig, G. Lumay, H. Caps, N. Vandewalle, S. Rondia, M. Mélard, J. van Loon, A. Dowson, and S. Vincent-Bonnieu, Influence of the gravity on the discharge of a silo, *Granular Matter*, **15**, 263–273 (2013).
- [37] D. López-Rodríguez, D. Gella, K. To, D. Maza, A. Garcimartín, and I. Zuriguel, Effect of hopper angle on granular clogging, *Phys. Rev. E*, **99**, 032901 (2019).